Preventive Veterinary Medicine 98 (2011) 99–110

Contents lists available at ScienceDirect

Preventive Veterinary Medicine

journal homepage: www.elsevier.com/locate/prevetmed

Simulation of the seasonal cycles of bird, equine and human West Nile virus cases

Vincent Laperriere, Katharina Brugger, Franz Rubel*

Institute for Veterinary Public Health, University of Veterinary Medicine Vienna, Veterinärplatz 1, A-1210 Vienna, Austria

ARTICLE INFO

Article history:
Received 23 August 2010
Received in revised form 22 October 2010
Accepted 25 October 2010

Keywords:
Zoonosis
Arbovirus
Infectious disease
West Nile virus
Epidemic model
Climate forcing
Temperature dependent parameters
Seasons

ABSTRACT

The West Nile virus (WNV) is an arthropod-borne virus (arbovirus) circulating in a natural transmission cycle between mosquitoes (enzootic vectors) and birds (amplifying hosts). Additionally, mainly horses and humans (dead-end hosts) may be infected by blood-feeding mosquitoes (bridge vectors). We developed an epidemic model for the simulation of the WNV dynamics of birds, horses and humans in the U.S., which we apply to the Minneapolis metropolitan area (Minnesota). The SEIR-type model comprises a total of 19 compartments, that are 4 compartments for mosquitoes and 5 compartments or health states for each of the 3 host species. It is the first WNV model that simulates the seasonal cycle by explicitly considering the environmental temperature. The latter determines model parameters responsible for the population dynamics of the mosquitoes and the extrinsic incubation period. Once initialized, our WNV model runs for the entire period 2002–2009, exclusively forced by environmental temperature. Simulated incidences are mainly determined by host and vector population dynamics, virus transmission and herd immunity, respectively.

We adjusted our WNV model to fit monthly totals of reported bird, equine and human cases in the Minneapolis metropolitan area. From this process we estimated that the proportion of actually WNV-induced dead birds reported by the *Centers for Disease Control and Prevention* is about 0.8%, whereas 7.3% of equine and 10.7% of human cases were reported. This is consistent with referenced expert opinions whereby about 10% of equine and human cases are symptomatic (the other 90% of asymptomatic cases are usually not reported). Despite the restricted completeness of surveillance data and field observations, all major peaks in the observed time series were caught by the simulations. Correlation coefficients between observed and simulated time series were $R = 0.75$ for dead birds, $R = 0.96$ for symptomatic equine cases and $R = 0.86$ for human neuroinvasive cases, respectively.

1. Introduction

Goal of this paper is to adapt the existing theoretical framework of epidemic modeling to prove our understanding of the West Nile virus (WNV) dynamics. Therefore multiple seasonal cycles of bird, equine and human WNV cases in the Minneapolis metropolitan area (MN, U.S.) were simulated in order to demonstrate that our explanatory model is able to reproduce observations.

Since their emergence at the American continent in 1999, the West Nile virus encephalitis, a mosquito-born zoonotic disease, is in the centre of attention of the scientific community. An overview on the WNV epidemics in the U.S. was given for example by Petersen and Roehrig (2001) or Hayes et al. (2005). Beside these reviews more than 4,000 peer reviewed papers from various scientific disciplines were published. Some authors proposed statistical relationships between environmental parameters and WNV

* Corresponding author. Tel.: +43 1 25077 3532; fax: +43 1 25077 3590.
E-mail address: Franz.Rubel@vetmeduni.ac.at (F. Rubel).

0167-5877/$ – see front matter © 2010 Elsevier B.V. All rights reserved.
doi:10.1016/j.prevetmed.2010.10.013

dynamics. Based on this assumptions, descriptive models, mostly connected to geographical information systems (GIS), were presented in order to provide statistical predictors for possible WNV outbreaks. For example, statistical investigations of the WNV epidemics in the Minneapolis metropolitan area were recently presented by Ghosh and Guha (2010). More sophisticated epidemic models preferably should be developed which may be used to investigate further hypotheses on WNV transmission. However, until today no such mechanistic (explanatory) models were applied to simulate long time series of WNV cases in birds, horses and humans. This is remarkable, because firstly the theory was presented in a lot of papers as discussed below and secondly surveillance data for verification are easily available, provided for example by the *Centers for Disease Control and Prevention* (CDC, 2010).

The first epidemic model for vector-borne diseases was presented in 1908 by Ronald Ross and is today well-known as Ross–Macdonald malaria model (Ross, 1911; Macdonald, 1957). Recent models extended the application and theory to a wide range of insect-borne diseases. The simulation of the seasonal cycle was incorporated implicitly by vector populations fluctuating in time like a sinusoidal curve or explicitly by using temperature dependent parameters for the mosquito life cycle and the extrinsic incubation period. The first was demonstrated for African horse sickness (Lord et al., 1996), the latter, for example, was applied to bluetongue disease (Gubbins et al., 2008) and Usutu virus epidemics (Rubel et al., 2008).

The first WNV model was presented by Thomas and Urena (2001) to investigate the effectivity of pesticide spraying to reduce mosquito populations and in succession human WNV encephalitis in New York city after the outbreak in late summer 1999. Another WNV model was presented by Wonham et al. (2004), who suggested a theoretical framework including the derivation of the basic reproduction number R_0. A similar WNV model was presented in a further theoretical study by Cruz-Pacheco et al. (2005). Their numerical results comprise the influence of mosquito vertical transmission on the WNV dynamics and estimated R_0 values for 8 common bird species. Bowman et al. (2005) extended the mosquito–bird transmission cycle by 5 compartments for humans including hospitalization of WNV patients. This work also focused on the derivation of R_0. Because the different WNV models result in different R_0 estimates, Wonham et al. (2006) compared the models discussed above with respect to their transmission assumptions. An age-structured WNV model was applied to the WNV dynamics in Southern Europe and Western Africa by Durand et al. (2010). A common feature of all existing WNV models is that they are formulated with constant parameters. Therefore, they are not able to describe the observed seasonal cycles of WNV cases and, consequently, have never been compared or verified with surveillance data.

Here we contribute to the solution of the above mentioned shortcomings by adapting and enhancing the epidemic model developed by Rubel et al. (2008) to explain the Usutu virus (USUV) epidemics in Vienna, Austria. Because USUV is closely related to WNV (Weissenböck et al., 2002), both vectors (mainly Culex mosquitoes) and hosts (birds) have similar population dynamics and the areas of investigation (USUV in Vienna and WNV in Minneapolis) are located in comparable climate zones (Kottek et al., 2006), the natural bird–mosquito transmission cycle of the USUV model was adapted almost unmodified for the WNV model. Population data of birds, horses and humans were adjusted for the Minneapolis metropolitan area. Temperature dependent mosquito parameters introduced by Rubel et al. (2008), however, remain unchanged and are therefore only briefly discussed.

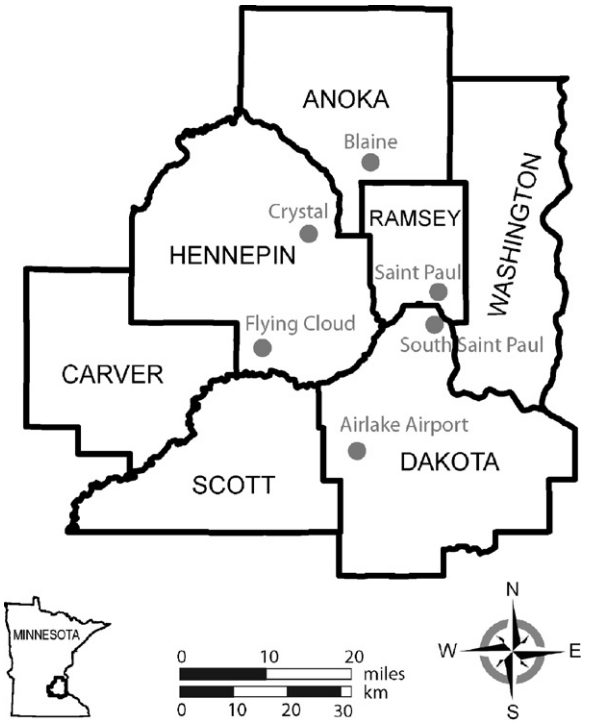

Fig. 1. Minneapolis metropolitan area (MN, U.S.) covering an area of 7280 km^2 (USCB, 2010b). Grey dots depict the locations of 6 meteorological stations with temperature measurements provided by the National Climate Data Center (NCDC, 2010).

2. Investigation area and data

In Minnesota, West Nile virus was for the first time detected in July 2002 when two dead crows, one from Hennepin County and one from Mille Lacs County, were tested positive. The first human and equine cases followed soon after these first reported dead birds (MDH, 2003). During the period 2002–2009 a total of 79% of the dead birds reported in Minnesota were found inside the Minneapolis metropolitan area (Fig. 1), which represents 3.4% of the area of the whole State. We thus restricted our analysis to this well sampled area, which totalizes 18.5% of the human and 16.0% of the equine cases in Minnesota, respectively.

2.1. Epidemiological data

Monthly accumulated dead birds as well as human and equine cases from the ArboNET surveillance program (CDC,

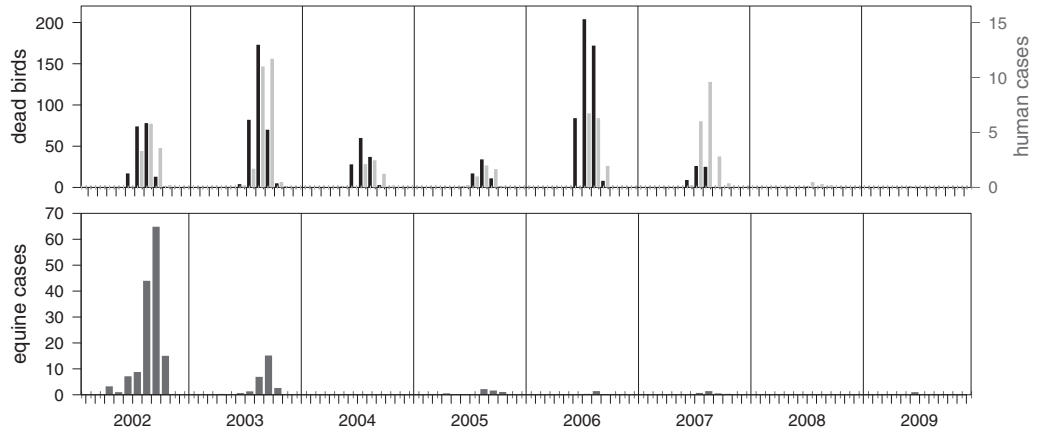

Fig. 2. Time series of monthly accumulated West Nile virus surveillance data compiled from (USGS, 2010b). Upper panel: observed dead birds (black) and human cases (grey). Lower panel: Equine cases. Period 2002–2009.

2010) have been compiled for this study. As depicted in Fig. 2 the temporal distribution of human cases match that of dead birds with the two epidemic peaks in 2003 and 2006 (correlation coefficient $R = 0.73$). A total of 92% of the human cases was reported between July and September. Equine cases follow a different pattern and are poorly correlated with dead birds ($R = 0.20$). They rapidly decrease after the first epidemic season in 2002, which accounts for a large majority (79%) of equine cases reported over 2002–2009. Equine vaccination, which has been practiced since 2002, has been hypothesized to be responsible, at least partially, for the decrease of incidence in equine cases (Dauphin and Zientara, 2007), while at the same time the number of human cases continued to grow. Although both experimental and observational studies have proved vaccination has beneficial effects regarding infection and death caused by WNV at an individual level (Schuler et al., 2004; Gardner et al., 2007), a quantitative investigation of its specific contribution to the decrease of equine WNV incidence compared to disease-induced immunity was outstanding and will be briefly addressed by our simulations.

2.2. Environmental data

As mentioned above, our WNV model is forced by environmental temperature data in order to reproduce and explain observed multi-seasonal dynamics of WNV infections in the Minneapolis metropolitan area. We used daily air–temperature measurements from 6 climate stations located within the study area (Fig. 1) which were provided by *National Climate Data Center* (NCDC, 2010). Firstly, we averaged this 6 station records to get mean temperatures representative for the entire model domain (Fig. 3, grey line). In a second step we averaged the daily values to monthly values to account for the temporal scale of both, the epidemiological data and the WNV model. The latter is designed to simulate monthly values and should therefore also be forced with monthly data. The simulating of

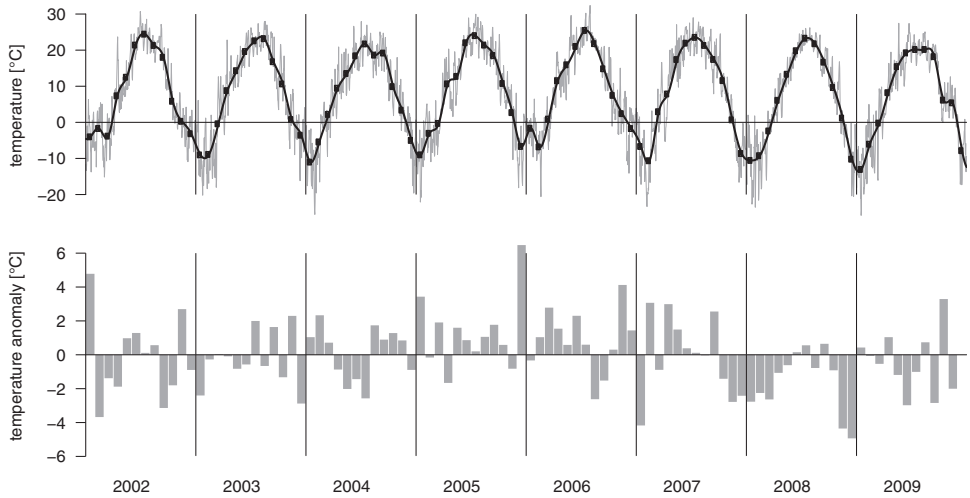

Fig. 3. Time series of observed temperatures averaged from 6 stations in the Minneapolis metropolitan area provided by the *National Climate Data Center* (NCDC, 2010). Upper panel: Daily (grey) and monthly (black) temperatures in degree Celsius. Lower panel: Monthly temperature anomalies in degree Celsius (deviations from monthly means of the period 2002–2009).

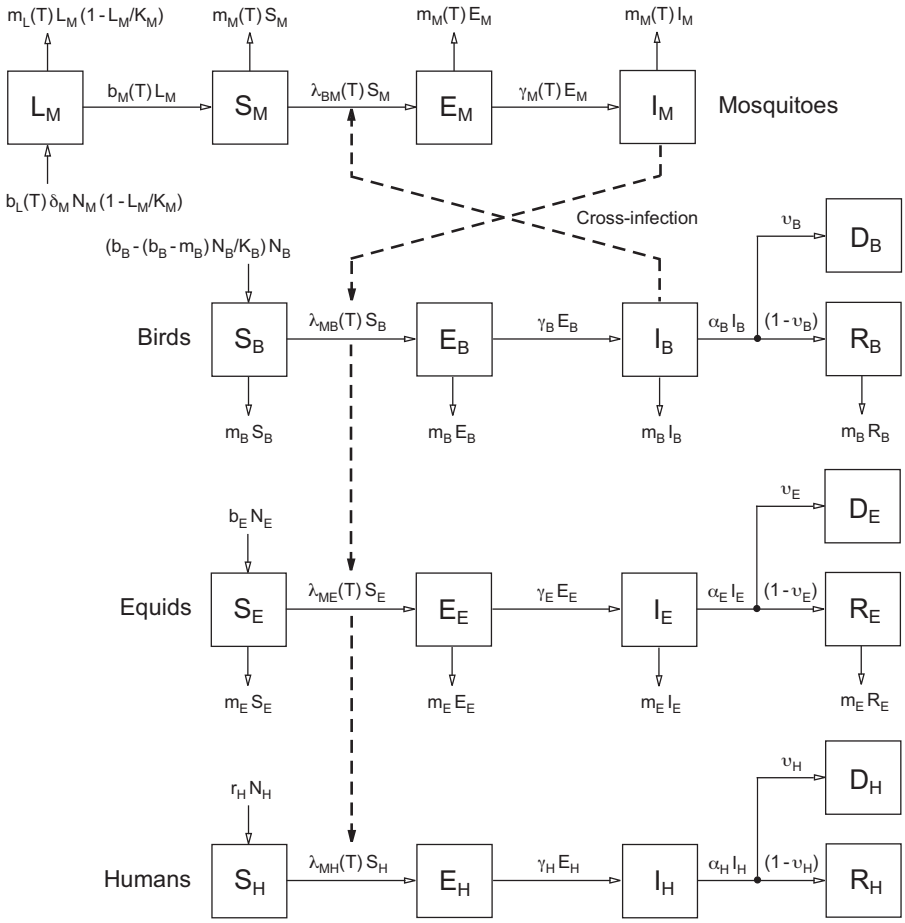

Fig. 4. Block diagram of the WNV model depicting the natural transmission cycle between mosquitoes and birds as well as the infection of the dead-end hosts equids (horses) and humans.

daily fluctuations would require a more comprehensive framework for the modeling of the mosquito population. Despite forcing and verification data are used at a monthly time scale, the numerical solution of the model equations require time steps of at least one day to ensure numerical stability. Therefore, we applied a spline function to interpolate the monthly averaged temperatures to the model time step (Fig. 3, black line).[1]

Additionally, a time series of monthly temperature anomalies is given in Fig. 3, lower panel. As discussed by Rubel et al. (2008) high USUV incidence in wild birds may be triggered by positiv temperature anomalies. Such a clear relation is not detectable in the WNV time series investigated in this study. At the best, positiv temperature anomalies in 2006 may be related to human symptomatic cases. The epidemic peak in 2003, however, may hardly be explaind by temperature anomalies alone.

[1] Note <fn0005>that forcing the WNV model with measured daily temperatures lead to similar results than using the theoretically more consistent monthly temperatures which were interpolated to the time step of the WNV model. The latter was proved to be at least one day, but may be shorter for other applications.

3. West Nile virus model

Our WNV model is based on the USUV model developed by Rubel et al. (2008). It is a SEIR (susceptible, exposed, infectious, removed) model simulating the seasonal lifecycles of birds, here American crows (*Corvus brachyrhynchos*), mosquitoes (*Culex* spp.) and the inter-specific WNV infection cycle between birds and mosquitoes. For a detailed description of the model we refer to Rubel et al. (2008). Here, we extended the basic model by the infection of the dead-end hosts horses and humans (Fig. 4). The WNV model has 19 compartments (i.e. health states). These comprise 4 health states for mosquito vectors (larvae L_M, susceptible mosquitoes S_M, exposed or latent-infected mosquitoes E_M and infectious mosquitoes I_M), 5 compartments for amplifying hosts, birds (susceptible birds S_B, exposed birds E_B, infectious birds I_B, recovered or immune birds R_B, dead birds D_B) as well as 5 health states for each of the dead-end hosts, horses, here referred to as equids (S_E, E_E, I_E, R_E and D_E), and humans (S_H, E_H, I_H, R_H, and D_H). In this study we do not investigate WNV-induced mortality in equids and humans. Nevertheless, to provide a complete WNV model, we differentiate between recovered (immune) and dead equids and humans instead to imple-

ment only one state, called removed. The latter denotes those hosts which do not further contribute to the infection process. They are determined by the removal rates α which is splitted into immune and dead states by the fraction ν. Further rates determining the health states are forces of infections λ and virus reproduction rates (reciprocals of the incubation periods) γ. Natural birth and mortality rates are denoted by b and m. Due to low WNV prevalence in humans, their population dynamics is simplified using an exponential growth model formulated with the reproduction rate $r = b - m$.

The WNV model depicted by the block diagram in Fig. 4 is described by 19 ordinary differential equations (ODEs); these are ODEs for 4 health states of mosquitoes

$$\frac{dL_M}{dt} = (b_L(T)\delta_M N_M - m_L(T)L_M)\left(1 - \frac{L_M}{K_M}\right) - b_M(T)L_M \quad (1)$$

$$\frac{dS_M}{dt} = -\lambda_{BM}(T)S_M + b_M(T)L_M - m_M(T)S_M \quad (2)$$

$$\frac{dE_M}{dt} = \lambda_{BM}(T)S_M - \gamma_M(T)E_M - m_M(T)E_M \quad (3)$$

$$\frac{dI_M}{dt} = \gamma_M(T)E_M - m_M(T)I_M \quad (4)$$

for 5 health states of birds

$$\frac{dS_B}{dt} = \left(b_B - (b_B - m_B)\frac{N_B}{K_B}\right)N_B - \lambda_{MB}(T)S_B - m_B S_B \quad (5)$$

$$\frac{dE_B}{dt} = \lambda_{MB}(T)S_B - \gamma_B E_B - m_B E_B \quad (6)$$

$$\frac{dI_B}{dt} = \gamma_B E_B - \alpha_B I_B - m_B I_B \quad (7)$$

$$\frac{dR_B}{dt} = (1 - \nu_B)\alpha_B I_B - m_B R_B \quad (8)$$

$$\frac{dD_B}{dt} = \nu_B \alpha_B I_B \quad (9)$$

for 5 health states of equids

$$\frac{dS_E}{dt} = b_E N_E - \lambda_{ME}(T)S_E - m_E S_E \quad (10)$$

$$\frac{dE_E}{dt} = \lambda_{ME}(T)S_E - \gamma_E E_E - m_E E_E \quad (11)$$

$$\frac{dI_E}{dt} = \gamma_E E_E - \alpha_E I_E - m_E I_E \quad (12)$$

$$\frac{dR_E}{dt} = (1 - \nu_E)\alpha_E I_E - m_E R_E \quad (13)$$

$$\frac{dD_E}{dt} = \nu_E \alpha_E I_E \quad (14)$$

and for 5 health states of humans

$$\frac{dS_H}{dt} = r_H N_H - \lambda_{MH}(T)S_H \quad (15)$$

$$\frac{dE_H}{dt} = \lambda_{MH}(T)S_H - \gamma_H E_H \quad (16)$$

$$\frac{dI_H}{dt} = \gamma_H E_H - \alpha_H I_H \quad (17)$$

$$\frac{dR_H}{dt} = (1 - \nu_H)\alpha_H I_H \quad (18)$$

$$\frac{dD_H}{dt} = \nu_H \alpha_H I_H \quad (19)$$

Eqs. (1)–(19) are solved numerically and require the estimation of the model parameters, i.e. the population parameters (natural birth and mortality rates), transition rates (forces of infection), virus reproduction rates (reciprocal of incubation periods), recovery rates, WNV-induced death rates as well as the specification of the initial conditions.

3.1. Disease-free population growth

Both mosquitoes and birds follow multi-seasonal disease-free dynamics by considering density dependent growth rates. We applied standard logistic growth models (Rubel et al., 2008). While the mosquito model comprises two compartments: one for the aquatic stages (eggs, larvae and pupae), called "Larvae" L_M, and one for the terrestrial stages, that is the total number of adults N_M, the bird models comprises only one compartment for the total number of birds N_B. In this process b_L, b_M and b_B denote the birth rates of larvae (egg-deposition rate), adults mosquitoes (maturation rate) and birds, respectively. Further, m_L, m_M and m_B are the natural mortality rates of larvae, adult mosquitoes and birds. Population densities are bounded by carrying capacities K_B and K_M, respectively. From American crow density in the study area we estimated the carrying capacity of birds as the total number of birds N_B in a disease free population as $K_B = 110{,}000$ birds (see Section 4.1). The carrying capacity of mosquito larvae was estimated as $K_M = 3{,}300{,}000$ (see Section 5). The seasonal cycle of the mosquito population is a consequence of temperature-dependent mosquito birth and mortality rates. Finally, the hibernation of adult mosquitoes (diapause) is considered by δ_m, the fraction of non-diapausing mosquitoes determined by the photoperiod at the geographical latitude of Minneapolis ($\varphi \simeq 45^\circ$ N). Again, further details are described by Rubel et al. (2008).

For equids and humans, however, we applied density independent population dynamics using parameters specified from livestock census (USDA, 2010) and population census (USCB, 2010b).

3.2. Infection and cross-infection processes

Birds and mosquitoes are connected by the cross-infection between the two species, whereas equids and humans are incidental or dead-end hosts. The latter may become infected with WNV, but do not contribute to further virus transmission. We applied temperature dependent forces of infection from birds to mosquitoes $\lambda_{BM}(T)$ and from mosquitoes to birds $\lambda_{MB}(T)$, equids $\lambda_{ME}(T)$ and humans $\lambda_{MH}(T)$, respectively. They were defined as frequency-dependent processes, following a concept initially proposed for malaria by Macdonald (1957).

$$\lambda_{BM}(T) = \delta_M k(T) p_B \frac{I_B}{K_B} \quad (20)$$

$$\lambda_{MB}(T) = \delta_M k(T) p_M \phi_B \frac{I_M}{K_M} \quad (21)$$

Table 1
Model parameters: Per capita rates in units days^{-1} and fractions for mosquitoes, birds, equids and humans. Mosquito rates $b_L(T)$, $m_L(T)$, $b_M(T)$, $m_M(T)$, $k(T)$ and $\gamma_M(T)$ are functions of the temperature T (Table 2). The fraction of non-diapausing mosquitoes $\delta_M(D)$ is a function of daytime length D and the birth rate of birds $b_B(d)$ is a function of the calendar day d (Fig. 4), respectively. All parameters were estimated from literature, except the unknown mosquito-to-host ratios ϕ_B, ϕ_E and ϕ_H which were determined by the model calibration.

Parameter	Value	Interpretation	Parameter	Value	Interpretation
b_L	$f(T)$	Birth rate, larvae			
m_L	$f(T)$	Mortality rate, larvae			
b_M	$f(T)$	Birth rate, mosquitoes	b_B	$f(d)$	Birth rate, birds
m_M	$f(T)$	Mortality rate, mosquitoes	m_B	0.00034	Mortality rate, birds
p_M	1.0	Transmission probability by infectious mosquitoes	p_B	0.125	Transmission probability by infectious birds
			α_B	0.4	Removal rate, birds
γ_M	$f(T)$	Rate with $1/\gamma_M$ extrinsic-incubation period	γ_B	1.0	Rate with $1/\gamma_B$ intrinsic-incubation period
δ_M	$f(D)$	Fraction mosquitoes non-diapausing	ν_B	0.7	Fraction birds dying due to infection
k	$f(T)$	Mosquito biting rate	ϕ_B	30	Mosquito-to-bird ratio
b_E	0.00016	Birth rate, equids	b_H	0.000055	Birth rate, humans
m_E	0.00011	Mortality rate, equids	m_H	0.000034	Mortality rate, humans
α_E	0.2	Removal rate, equids	α_H	0.5	Removal rate, humans
γ_E	0.05	Rate with $1/\gamma_E$ equid incubation period	γ_H	0.25	Rate with $1/\gamma_H$ human incubation period
ν_E	0.04	Fraction equids dying due to infection	ν_H	0.004	Fraction humans dying due to infection
ϕ_E	300	Mosquito-to-equid ratio	ϕ_H	0.03	Mosquito-to-human ratio

$$\lambda_{ME}(T) = \delta_M k(T) p_M \phi_E \frac{I_M}{K_M} \tag{22}$$

$$\lambda_{MH}(T) = \delta_M k(T) p_M \phi_H \frac{I_M}{K_M} \tag{23}$$

According to this, $\lambda_{BM}(T)$ is a function of the temperature dependent biting rate of mosquitoes $k(T)$ and the transmission probability p_B, that an infectious bird infects a susceptible mosquito. From mosquitoes to hosts, the forces of infection depend not only on $k(T)$ and the transmission probability p_M (assumed to be identical for birds, equids and humans), but also on the mosquito-to-host ratio given by parameters ϕ_B, ϕ_E and ϕ_H, respectively. On average a species receives $k(T)\phi_B$, $k(T)\phi_E$ or $k(T)\phi_H$ bites per unit of time. Frequency-dependence is considered here as the dependence of the force of infection on the fraction of infectious subjects with respect to the maximal density (the carrying capacity K_B or K_M) for the species considered. Because all epidemic terms comprise mosquito densities, they are multiplied by the fraction of non-diapausing mosquitoes δ_M to account for mosquito hibernation (Rubel et al., 2008).

4. Parameter estimation

Model parameters applied in our WNV model are summarized in Table 1. Thereby mosquito parameters (*Culex pipiens* complex) are taken unchanged from the USUV model of Rubel et al. (2008), because in fact they were estimated from mosquitoes in the U.S. or data on WNV. Bird parameters were adapted for amplifying bird hosts in Minnesota and parameters for equids and humans are specified from literature and U.S. census data.

4.1. Parameters for amplifying hosts: birds

Most of dead birds reported in the Minneapolis metropolitan area were American crows (*C. brachyrhynchos*). The analysis of avian morbidity and mortality data indicated that it was the most WNV sensitive bird species in northern regions (McLean, 2002; Yaremych et al., 2004). Therefore, we focused our simulations on this single species, although some recent studies suggested that corvids could be relatively unimportant in WNV amplification compared to some other species like American robins (Hamer et al., 2009).

Referenced American crow abundance data indicate densities of 10–20 birds/km^2. For example, Farnsworth et al. (2005) estimated a crow density of 18 birds/km^2 from a point count survey along some North-American *Breeding Bird Survey* (BBS) routes. Considering these converging information, we took 15 birds/km^2 for our study area of 7280 km^2 to estimate a carrying capacity of $K_B = 110{,}000$ birds. Although a wild crow was recorded living for over 14 years (Clapp et al., 1983), a mean lifespan of 8 years is the norm. Therefore, we determined a mortality rate of $m_B = 1/8 = 0.125$ years^{-1} corresponding to $m_B = 0.00034$ days^{-1}. The birth rate was estimated from a study of Chamberlain-Auger et al. (1990), who reported a reproductive success of 2.0 (range 0.8–3.3) surviving fledglings in average per pair of American crows. We applied this observed value in the model, yielding a per capita birth rate of $b_B = 1.0$ years^{-1} or $b_B = 0.0027$ days^{-1}. As depicted in Fig. 5, a gamma distribution was fitted to the observed frequency density distribution of the time of hatching (bars) by minimizing the residual sum-of-squares. The parameters of the gamma distribution were determined as $\alpha = 86.4$ and $\beta = 1.4$. Because the average annual birth rate $b_B = 1.0$ years^{-1}, the fitted gamma distribution (Eq. (24)) may be directly applied to describe the seasonal cycle of b_B as function of the calendar day d.

$$b_B = \frac{(d/\beta)^{\alpha-1}\exp(-d/\beta)}{\beta\Gamma(\alpha)}, \quad d, \alpha, \beta > 0 \tag{24}$$

From experimental infections, it has been shown that the average incubation period for American crows is about 1.8 days, range 1.0–3.0 (Komar et al., 2003; Brault et al., 2004). We specified $\gamma_B = 1.0$ days^{-1}. The mean duration of

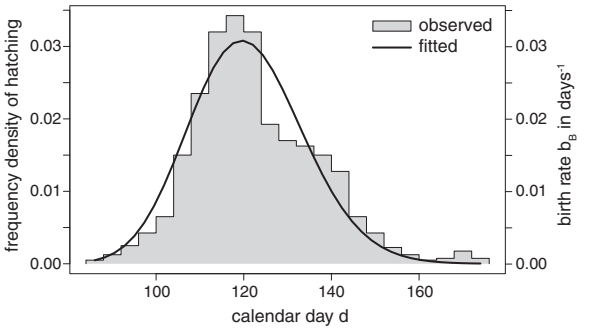

Fig. 5. Observed relative frequency of crow hatching after (Graber et al., 1987), temporal adjusted for Minneapolis. The fitted gamma distribution is used to specify the seasonal cycle of bird birth rate $b_B(d)$.

infectious level viremia in experimentally infected American crows has been estimated, for example, by Komar et al. (2003) to be 3.25 days. Generally, the infectious period of crows varies in the range of several days. We specified an infectious period of 2.5 days yielding a bird removal rate of $\alpha_B = 1/2.5 = 0.4\,\text{days}^{-1}$.

Information on WNV-induced bird mortality is obtained from surveillance reporting data, from captive and free ranging field studies, and from experimental infection studies (McLean, 2006). While in laboratory experiments mortality was 100% (Komar et al., 2003; Brault et al., 2004), under field conditions an overall mortality of 43% of American crows was observed (McLean, 2006). The highest mortality was observed in central Illinois, where 68% of radiotagged American crows died from confirmed WNV infection (Yaremych et al., 2004). In New York and in Oklahoma, however, only 37% and 40% of American crows died in 2002 (Caffrey et al., 2003). Considering the wide range of WNV-induced crow mortality, we roughly determined the fraction of dead birds as $\nu_B = 0.7$.

Finally, according to Rubel et al. (2008), we assume that infectious birds transmit the virus with a probability of $p_B = 0.125$ to blood-feeding mosquitoes.

4.2. Parameters for dead-end hosts: equids and humans

Annually time series of the human population of the Minneapolis metropolitan area are provided by USCB (2010a). According to this, the population increases from 2002 to 2009 by about 150,000 people. Starting with $N_H = 2{,}700{,}000$ humans in 2002, we calculated a human reproduction rate of $r_H = b_H - m_H = 0.000021\,\text{days}^{-1}$ by fitting an exponential growth model (not shown). From an average human life time of about 80 years (McMurry, 2002), we get $m_H = 0.000034\,\text{days}^{-1}$, leading to $b_H = 0.000055\,\text{days}^{-1}$. Note that b_H is called birth rate but includes immigration as well. The total number of horses of $N_E = 10,700$ is taken from the 2002 census of USDA (2010). Assuming an average life time for horses of about 25 years we get $m_E = 0.00011\,\text{days}^{-1}$. As for humans, increasing equine population is considered by $b_E = 0.00016\,\text{days}^{-1}$.

The human incubation period is usually referenced with 2–15 days (Center for Food Security and Public Health, 2009). The equine incubation period is also not well known, but might be slightly longer. We specified $\gamma_H = 1/4 = 0.25\,\text{days}^{-1}$ and $\gamma_E = 1/20 = 0.05\,\text{days}^{-1}$.

Table 2
Mosquito parameters as functions of temperature T in °C and hibernation as function of daytime length D in hours form Rubel et al. (2008).

Parameter	Function
b_L	$f(T) = 0.7998/[1 + 1.231\exp(-0.184(T-20))]$
m_L	$f(T) = 0.0025T^2 - 0.094T + 1.0257$
b_M	$f(T) = b_L(T)/10$
m_M	$f(T) = m_L(T)/10$
k	$f(T) = 0.344/[1 + 1.231\exp(-0.184(T-20))]$
γ_M	$f(T) = 0.0093T - 0.1352$, for $T > 15$ °C, else $\gamma_M(T) = 0$
δ_M	$f(D) = 1 - 1/[1 + 1775.7\exp(1.559(D-18.177))]$

Contrary to American crows, most of equids and humans do not show clinical signs or are only mildly affected by the infection. Fatal cases are significantly lower than for American crows. The clinical attack rate in horses with either experimental or natural infection is about 10%, while around 90% of cases are asymptomatic (Komar, 2000; Bunning et al., 2002). Without any treatment, mildly affected horses generally recover in 2–7 days (Trock et al., 2001), even though this period can be extended to several weeks. For our simulations we applied a removal rate of $\alpha_E = 1/5 = 0.2\,\text{days}^{-1}$. According to the Center for Food Security and Public Health (2009), 30–40% of horses who develop symptoms will die from the infection. Cantile et al. (2001) estimated a value of 38%. We applied a global fraction of fatal equine cases of $\nu_E = 0.1 \cdot 0.4 = 0.04$, which is approximately one order of magnitude lower than for birds.

Between 1999 and 2005 a total number of 20,000 neuroinvasive human WNV cases as well as 770 WNV-induced death were reported in the entire area of the U.S. The effective number of WNV cases in humans is unknown, but was assumed to be about 215,000 (Hayes et al., 2005). Thus, the fraction of fatal human cases may be roughly estimated as $\nu_H = 770/215{,}000 = 0.0036 \simeq 0.004$. The human removal rate is set to $\alpha_H = 0.5\,\text{days}^{-1}$, knowing that the duration of clinical signs of patients vary within a wide range (Watson et al., 2004). Because humans do not contribute to the natural WNV transmission cycle, the simulations are not very sensitive with regard to the specification of α_H.

5. Numerical implementation, initialization and calibration

The WNV model is implemented with the statistical computing language R (R Development Core Team, 2010) and solved numerically. Therefore, Eqs. (1)–(19) are discretized using the Euler–Cauchy method with a time step of 1 day to assure numerical stability.

Once initialized with some infectious mosquitoes, our model simulates mosquito and host health states for the entire period 200–2009 without further input of epidemiological data. It is forced exclusively by the environmental temperature via the temperature-dependent mosquito parameters described in Table 2. Thus, we started with completely susceptible host populations, specified by census data, into which we introduced a pre-specified number of infectious mosquitoes (Table 3).

Because our simulation starts in wintertime, the initial value of mosquito larvae are set to zero and the number of

Table 3
Model initial values for mosquito, bird, equine and human health states. While susceptible birds, equids and humans were taken from census 2002, the number of initially susceptible and infectious mosquitoes was estimated by calibration. All other health states are initially zero. Note that susceptible mosquitoes reflect the minimum population in winter, while the number of initially susceptible birds is equal to the maximum, the carrying capacity $K_B = 110,000$. Mosquito larvae are bounded by $K_M = 3,300,000$.

Health state	Initial value	Interpretation
$S_{M,0}$	500,000	Susceptible mosquitoes, $S_{M,0} = N_{M,\min}$
$S_{B,0}$	110,000	Susceptible birds, $S_{B,0} = N_{B,0} = K_B$
$S_{E,0}$	10,700	Susceptible equids, $S_{E,0} = N_{E,0}$
$S_{H,0}$	2,700,000	Susceptible humans, $S_{H,0} = N_{H,0}$
$I_{M,0}$	100	Infectious mosquitoes

susceptible mosquitoes is specified by the number of hibernating mosquitoes $N_{M,\min}$. This minimum number of adult mosquitoes is a constant, used in the model to avoid that simulated mosquitoes become extinct. The initial number of susceptible birds is set to the maximum bird population size $N_{B,0} = 110,000$ equal to the carrying capacity K_B. Susceptible equids, however, are initialized with census data from USDA (2010), which reported $N_{E,0} = 10,700$ horses in 2002. From USCB (2010b) we specified the initial number of humans living 2002 in the Minneapolis metropolitan area as $N_{H,0} = 2,700,000$.

Which number of infected mosquitoes should be introduced into completely susceptible host populations to start WNV-transmission of is rather unknown. Therefore we specified $I_{M,0} = 100$ during the calibration process. The calibration of the model was done by minimizing the root-mean-square error between observed and simulated time series of monthly bird, equine and human cases as depicted in Fig. 7. Here, we prefer this simple approach even though more sophisticated methods were investigated and applied by the authors (Reiczigel et al., 2010), because it leads to satisfying results. A total of 5 unknown parameters were specified by the calibration. These are the initial values $S_{M,0} = N_{M,min}$ and $I_{M,0}$ as well as the mosquito-to-bird ratio ϕ_B, the mosquito-to-equid ratio ϕ_E and mosquito-to-human ratio ϕ_H, respectively (Tables 1 and 3). The calibration process includes also an adjustment of our WNV model to fit it to monthly totals of reported bird, equine and human cases. This is necessary because only a proportion of actually WNV-induced dead birds as well as equine and human cases are reported by CDC (2010), while our WNV model simulates the total populations.

Practically, the calibration procedure was done as follows: In a first step we determined realistic ranges for each of the 5 unknown values, that are $S_{M,0}$, $I_{M,0}$, ϕ_B, ϕ_E and ϕ_H. In a second step the first possible parameter set was taken to run the model. Then the model results were scaled to the observations (equal sums of cases) and the mean-square error was calculated. Repeating the second step for all possible parameter sets results in an optimal estimate of the 5 unknown values via the minimal mean-square error. We specified initial values of $S_{M,0} = 500,000$ and $I_{M,0} = 100$ (Table 3). The mosquito-to-host ratios were determined as $\phi_B = 30$, $\phi_E = 300$ and $\phi_H = 0.03$ (Table 1). For all values we specified orders of magnitudes, which seems to be more reasonable than to apply 'exact' values. While our estimate of ϕ_B is similar to the value suggested by Wonham et al. (2004) who set $\phi_B = 100$, references for ϕ_E and ϕ_H are missing. Note that from $\phi_B = K_M/K_B$ ($K_B = 110,000$ from census), the unknown maximum mosquito population is calculated as $K_M = 3,300,000$. It is reasonable to assume that not all ornithophilic mosquitoes serve as bridge vectors. Therefore, the mosquito-to-equid ratio should be of the order of $\phi_E \leq K_M/N_E \approx 300$. From the calibration process, however, we also got $\phi_E = 300$, which indicates that all mosquitoes serve as bridge vectors for horses. The mosquito-to-human ratio should be $\phi_H \leq K_M/N_H \approx 1$. Because in urban environments humans are less exposed to mosquitoes we expect values of $\phi_H \ll 1$. This was confirmed by $\phi_H = 0.03$ as estimated by the model calibration process.

6. Results

Simulation results, i.e. time series of vector and host populations for the health states susceptible S, immune R and infectious I, are depicted in Fig. 6. While mosquito population dynamics is driven by climate (temperature), total bird population $N_B = E_B + I_B + R_B$ decreases due to WNV-induced deaths. At the same time the number of susceptible birds decreases too, due to increasing numbers of immune birds. Local peaks in bird time series are caused by the seasonal cycle of bird birth rates. In winter 2007/2008, a high proportion of American crows acquired immunity and the susceptible bird population reached its minimum value of about $S_B = 20,000$ birds. Total bird population decreases to $N_B = 60,000$ birds ($K_B = 110,000$).

WNV dynamics of equids is quite different. Due to the implementation of the reproduction rate estimated from livestock census, simulated equid population increases from $N_E = 10,700$ horses in 2002 to about $N_E = 12,000$ horses in 2009. After the major epidemic peaks in 2002 and 2003, nearly all equids (horses) acquired immunity. This high level of herd immunity in horses explains the low numbers of cases after 2003. Note that vaccination of horses started in 2002, but was not considered in our study because the fraction of vaccinated horses is not well documented. Nevertheless, even without considering vaccination, our simulations reproduce the reported equine symptomatic cases quite well (Fig. 7). This results are not astonishing, but lead to the question on the effectivity of the recent WNV vaccination of horse populations.

Human population dynamics is not essentially influenced by WNV, because of the low WNV prevalence in humans (note the logarithmic scaling of human health states in Fig. 6). The dynamics of human symptomatic cases follow the pattern of the mosquito dynamics and is also similar to the time series of reported dead crows.

A comparison of observed and simulated bird, equine and human cases is given in Fig. 7. For the verification we accumulated our daily simulations to monthly values as available for observations. Additionally, the WNV model output is scaled to the magnitude of the observations (equal sums of observations and simulations), because only a proportion of actually WNV-cases is reported. We estimated that the proportion of actually WNV-induced dead birds reported by CDC (2010) is about 0.8%, whereas 7.3% of equines and 10.7% of human cases were reported. This is

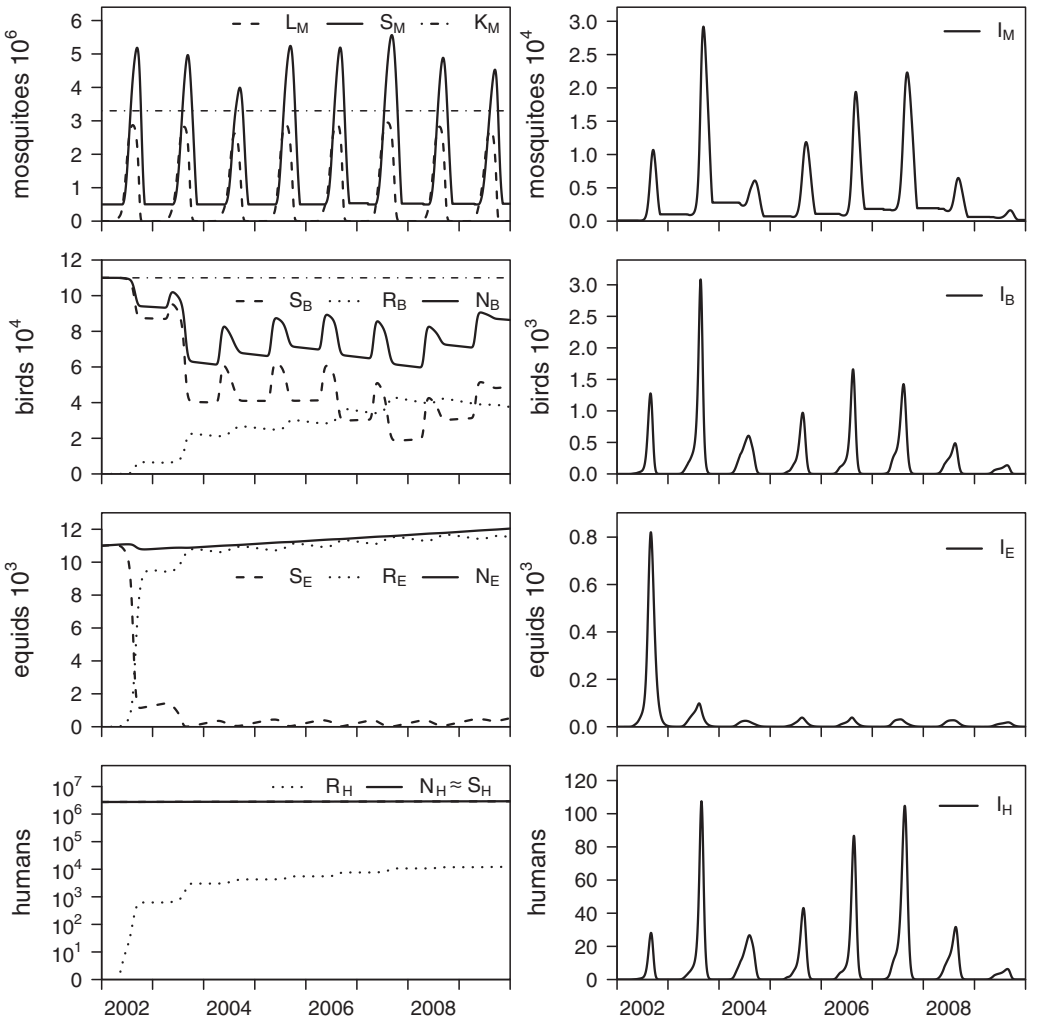

Fig. 6. Simulated time series of mosquito, bird, equine and human health states.

consistent with referenced values from expert opinions of about 10% symptomatic cases of horses and human which were reported (90% of asymptomatic cases are usually not reported). Our estimate of the dead birds reported, however, is one order of magnitude less than indicated by a field experiment performed by Ward et al. (2006) who found that the proportion of reported crows was 27.3% in urban area and 10.3% in rural area, respectively. Nevertheless, both estimates suggest that human density and associated factors can substantially influence dead crow reporting and, thus, the observed distribution of WNV. The correlation coefficient of $R = 0.75$ between observed and simulated dead birds should be evaluated with respect to the above mentioned findings. Especially the lower correspondence during the second half of the investigation period may be caused by a shift in the reporting rate due to a loss of the public's interest.

Significantly higher correlations were calculated for horses ($R = 0.96$) and humans ($R = 0.86$). Maybe this is an effect of the better reliability of equine and human surveillance data. Nevertheless, it should be noted that these good correlations do not reflect an independent model verification, but rather a demonstration of the skill of the WNV model to reproduce observations.

7. Discussion and outlook

In this paper we demonstrated for the first time the ability of epidemic models to reflect the WNV cases in birds, horses and humans in a specified study area. Our WNV model which comprises a total of 19 compartments (health states) and a multiplicity of parameters, many of them functions of the environmental temperature, is rather complex. However, it may be easy implemented on a personal computer. For demonstration purposes, the computer source code is provided to the scientific community at our website http://epidemic-modeling.vetmeduni.ac.at. The R-code (R Development Core Team, 2010) is only three pages long and may be used to recalculate our results, to simulate control strategies or to investigate further hypotheses associated with WNV transmission.

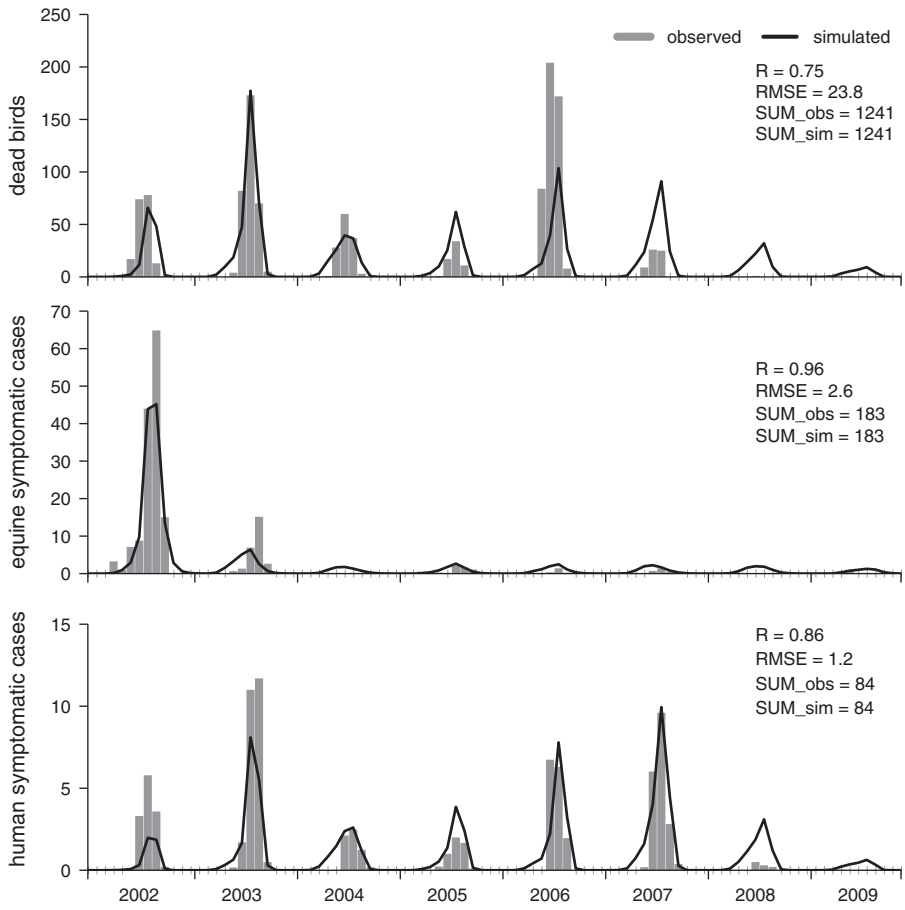

Fig. 7. Time series of observed and simulated dead crows (upper panel), equine cases (middle panel) and human cases (lower panel) in the Minneapolis metropolitan area. Simulations are adjusted to the scale of observations (equal sums). The WNV model explains time series of dead birds with a correlation of $R = 0.75$, although the second part of the time series of simulated birds exhibits certain qualitative deviation from the observations. Equine cases are correlated with $R = 0.96$, human cases with $R = 0.86$. Period 2002–2009.

Our simulations are based on the hypothesis that a WNV model, forced exclusively by temperature, is able to reproduce the observed WNV dynamics. Regarding human cases about 74% of the variation of the observations was reproduced by the simulation (correlation coefficient $R = 0.86$). To improve this explained variance, additional hypotheses may be implemented. These comprise, for example, the importance of additional bird species which may serve as amplifying hosts (Cruz-Pacheco et al., 2005). Also seasonality in mosquito feeding behavior as discussed by Fonseca et al. (2004) and Kilpatrick et al. (2006) may be considered. Additional forcing data, such as soil moisture, may be used to investigate a potential drought-induced amplification of the WNV dynamics as discussed by Shaman et al. (2005). Vice versa, an attenuation of the WNV dynamics due to the application of control measures to decrease vector population size (e.g. spraying) is not yet considered in our model as well.

A future challenge will be to extend WNV models by considering viral genetics. Unifying the epidemic and evolutionary dynamics of WNV is outstanding, although first general theoretical frameworks are available as reviewed by Grenfell et al. (2004) and Volz et al. (2009). The latter demonstrated the application of the phylodynamics of infectious diseases by means of HIV. In contrast, the consideration of the genetic and phenotypic variations of WNV will be a much simpler task. In 2001 the originally introduced WNV genotype NY99 was displaced by the genotype WN02, which was discussed to be accountable for the efficient spread across the U.S. (Ebel et al., 2004). This hypothesis was confirmed by the laboratory experiments of Kalipatrick et al. (2008), who showed that the fraction of mosquitoes infected with WN02 increases faster than those infected with NY99. The rapid expansion of WN02 is linked to a shorter extrinsic incubation period in Culex mosquitoes for low and high temperatures, respectively. Increasing WNV propagation velocity is depicted in the U.S. maps of human neuroinvasive disease incidence (Hayes et al., 2005) provided by CDC (2010). The velocity was low during the initial phase 1999–2001 and rapid thereafter. In our study, however, we do not account for different WNV genotypes, because WNV in Minnesota was for the first time reported in 2002.

Primarily we are interested to apply our model to other regions in the U.S. and, if successful, expand it to a spatial reaction-diffusion model as suggested in theoretical

papers, e.g. by Liu et al. (2006). Such a continental-scale spatial WNV model would open up the opportunity to quantitatively investigate the role of animal trade and migratory birds (Kenkre et al., 2005; Rappole et al., 2006; Pfeffer and Dobler, 2010). Forced with daily temperature fields from numerical weather prediction models, a 10 day forecast for the entire U.S. may be compiled. WNV dynamics according to future climate scenarios (Rubel and Kottek, 2010), however, may be estimated by forcing our WNV model with climate predictions as demonstrated for Usutu virus in Vienna, Austria (Brugger and Rubel, 2009).

A final verification of the skill of our WNV model to simulate or predict observations will be possible in some years when time series have been extended by new model independent surveillance data.

References

Bowman, C., Gumel, A.B., van den Driessche, P., Wu, J., Zhu, H., 2005. A mathematical model for assessing control strategies against West Nile virus. Bull. Math. Biol. 67, 1107–1133.

Brault, A.C., Langevin, S.A., Bowen, R.A., Panella, N.A., Biggerstaff, B.J., Miller, B.R., Komar, N., 2004. Differential virulence of West Nile strains for American crows. Emerg. Infect. Dis. 10, 2161–2168.

Brugger, K., Rubel, F., 2009. Simulation of climate-change scenarios to explain Usutu-virus dynamics in Austria. Prev. Vet. Med. 88, 24–31.

Bunning, M.L., Bowen, R.A., Cropp, C.B., Sullivan, K.G., Davis, B.S., Komar, N., Godsey, M.S., Baker, D., Hettler, D.L., Holmes, D.A., Biggerstaff, B.J., Mitchell, C.J., 2002. Experimental infection of horses with West Nile Virus. Emerg. Infect. Dis. 8, 380–386.

Caffrey, C., Weston, T., Smith, S., 2003. High mortality amond marked crows subsequent to the arrival of West Nile virus. Wildlife Soc. B 31, 870–872.

Cantile, C., Piero, F.D., Guardo, G.D., Arispici, M., 2001. Pathologic and immunohistochemical findings in naturally occuring West Nile virus infection in horses. Vet. Pathol. 38, 414–421.

CDC, 2010. Centers for Disease Control and Prevention: West Nile Virus—Statistics, Surveillance, and Control Archive. Available at: http://www.cdc.gov/ncidod/dvbid/westnile/surv&control.htm.

Center for Food Security and Public Health, 2009. West Nile Virus Infection. Available at: www.cfsph.iastate.edu/Factsheets/pdfs/west_nile_fever.pdf.

Chamberlain-Auger, J.A., Auger, P.J., Strauss, E.G., 1990. Breeding biology of American crows. Wilson Bull. 102, 615–622.

Clapp, R.B., Klimkiewicz, M.K., Futcher, A.G., 1983. Longevity records of North American birds: Columbidae through Paridae. J. Field Ornithol. 54, 123–137.

Cruz-Pacheco, G., Esteva, L., Montaño-Hirose, J.A., Vargas, C., 2005. Modelling the dynamics of West Nile Virus. Bull. Math. Biol. 67, 1157–1172.

Dauphin, G., Zientara, S., 2007. West Nile Virus: recent trends in diagnosis and vaccine development. Vaccine 25, 5563–5576.

Durand, B., Balanca, G., Baldet, T., Chevalier, V., 2010. A metapopulation model to simulate West Nile virus circulation in Western Africa, Southern Europe and the Mediterranean basin. Vet. Res. 41, 32, doi:10.1051/vetres/2010004.

Ebel, G.D., Carricaburu, J., Young, D., Bernard, K.A., Kramer, L.D., 2004. Genetic and phenotypic variation of West Nile virus in New York, 2000–2003. Am. J. Trop. Med. Hyg. 71, 493–500.

Farnsworth, G.L., Nichols, J.D., Sauer, J.R., Fancy, S.G., Pollock, K.H., Shriner, S.A., Simons, T.R., 2005. Statistical approaches to the analysis of point count data: a little extra information can go a long way. In: Ralph, C.J., Rich, T.D. (Eds.), Bird Conservation Implementation and Integration in the Americas, Proc. 3rd Int. Partners in Flight Conf. 20–24 March 2002, Asilomar, CA.

Fonseca, D.M., Keyghobadi, N., Malcolm, C.A., Mehmet, C., Schaffner, F., Mogi, M., Fleischer, R.C., Wilkerson, R.C., 2004. Emerging vectors in the *Culex pipiens* complex. Science 303, 1535–1538.

Gardner, I.A., Wong, S.J., Ferraro, G.L., Balasuriya, U.B., Hullinger, P.J., Wilson, W.D., Shi, P.-Y., MacLachlan, N.J., 2007. Incidence and effects of West Nile virus infection in vaccinated and unvaccinated horses in California. Vet. Res. 38, 109–116.

Ghosh, D., Guha, R., 2010. Use of genetic algorithm and neural network approaches for risk factor selection: a case study of West Nile virus dynamics in an urban environment. Comput. Environ. Urban Syst. 34, 189–203.

Graber, J.W., Graber, R.R., Kirk, E.L., 1987. Illinois Birds; Corvidae. Illinois Natural History Survey Biological Notes 126, 42 pp.

Grenfell, B.T., Pybus, O.G., Gog, J.R., Wood, J.N.L., Daly, J., Mumford, J.A., Holmes, E.C., 2004. Unifiying the ecological and evolutionary dynamics of pathogens. Science 303, 327–332.

Gubbins, S., Carpenter, S., Baylis, M., Wood, J.L.N., Mellor, P.S., 2008. Assessing the risk of bluetongue to UK livestock: uncertainty and sensitivity analyses of a temperature-dependent model for the basic reproduction number. J. R. Soc. Interf. 5, 363–371.

Hamer, G.L., Kitron, U.D., Goldberg, T.L., Brawn, J.D., Loss, S.R., Ruiz, M.O., Hayes, D.B., Walker, E.D., 2009. Host selection by *Culex pipiens* mosquitoes and West Nile virus amplification. Am. J. Trop. Med. Hyg. 80, 268–278.

Hayes, E.B., Komar, N., Nasci, R.S., Montgomery, S.P., O«Leary, D.R., Campbell, G.L., 2005. Epidemiology and transmission dynamics of West Nile virus disease. Emerg. Inf. Dis. 11, 1167–1173.

Kenkre, V.M., Parmenter, R.R., Peixoto, I.D., Sadasiv, L., 2005. A theoretical framework for the analysis of the West Nile virus epidemic. Comp. Math. Appl. 42, 313–324.

Kilpatrick, A.M., Daszak, P., Jones, M.J., Marra, P.P., Kramer, L.D., 2006. Host heterogeneity dominates West Nile virus transmission. Proc. R. Soc. B 273, 2327–2333.

Kilpatrick, A.M., Meola, M.A., Moudy, R.M., Kramer, L.D., 2008. Temperature, viral genetics, and the transmission of West Nile virus by *Culex pipiens* mosquitoes. PLoS Pathog. 4, e1000092, doi:10.1371/journal.ppat.1000092.

Komar, N., 2000. West Nile viral encephalitis. Rev. Sci. Tech. 19, 166–176.

Komar, N., Langevin, S., Hinten, S., Nemeth, N., Edwards, E., Hettler, D., Davis, B., Bowen, R., Bunning, M., 2003. Experimental infection of North American birds with the New York 1999 strain of West Nile virus. Emerg. Infect. Dis. 9, 311–322.

Kottek, M., Grieser, J., Beck, C., Rudolf, B., Rubel, F., 2006. World map of the Köppen-Geiger climate classification updated. Meteorol. Z. 15, 259–263.

Liu, R., Shuai, J., Wu, J., Zhu, H., 2006. Modeling spatial spread of West Nile virus and impact of directional dispersal of birds. Math. Biosci. Eng. 3, 145–160.

Lord, C.C., Woolhouse, M.E.J., Heesterbeek, J.A.P., Mellor, P.S., 1996. Vector borne diseases and the basic reproduction number: a case study of African Horse Sickness. Med. Vet. Entomol. 10, 19–28.

Macdonald, G., 1957. The Epidemiology and Control of Malaria. Oxford University Press, London.

McLean, R., 2006. West Nile virus in North American birds. Ornithol. Monogr. 60, 44–64.

McLean, R.G., 2002. West Nile virus: a threat to North American avian species. In: Rahm, J. (Ed.), Transactions of the Sixty-seventh North American Wildlife and Natural Resources Conference. Washington, DC.

McMurry, M., 2002. Minnesota Life Expectancy in 2000. Population Notes of the Minnesota Planning State Demograpic Center 95, 4 pp.

MDH, 2003. Minnesota Department of Health: West Nile Virus—an update for Minnesota medical providers. Disease Control Newsletter, 29–32.

NCDC, 2010. National Climatic Data Center: Global Summary of the Day (GSOD). Available at: http://www7.ncdc.noaa.gov/CDO/cdoselect.cmd?datasetabbv=GSOD.

Petersen, L.R., Roehrig, J.T., 2001. West Nile virus: a reemerging global pathogen. Emerg. Infect. Dis. 7, 611–614.

Pfeffer, M., Dobler, G., 2010. Emergence of zoonotic arboviruses by animal trade and migration. Parasites Vectors 3, 35. doi:10.1186/1756-3305r-r3-35.

R Development Core Team, 2010. R: A Language and Environment for Statistical Computing, R Foundation for Statistical Computing, Vienna, Austria, ISBN 3-900051-07-0. Version 2.11.1 Availabel at: http://www.R-project.org/.

Rappole, J.H., Compton, B.W., Leimgruber, P., Robertson, J., King, D.I., Renner, S.C., 2006. Modeling movement of West Nile virus in the western hemisphere. Vector-Borne Zoonotic Dis. 6, 128–139.

Reiczigel, J., Brugger, K., Rubel, F., Solymosi, N., Lang, Z., 2010. Bayesian analysis of a dynamical model for the spread of the Usutu virus. Stoch. Environ. Res. Risk Assess. 24, 455–462.

Ross, R., 1911. The Prevention of Malaria, 2nd ed. Murray, London.

Rubel, F., Brugger, K., Hantel, M., Chvala, S., Bakonyi, T., Weissenböck, H., Nowotny, N., 2008. Explaining Usutu virus dynamics in Austria: model development and calibration. Prev. Vet. Med. 85, 166–186.

Rubel, F., Kottek, M., 2010. Observed and projected climate shifts 1901–2100 depicted by world maps of the Köppen-Geiger climate classification. Meteorol. Z. 19, 135–141.

Schuler, L.A., Khaitsa, M.L., Dyer, N.W., Stoltenow, C.L., 2004. Evaluation of an outbreak of West Nile virus infection in horses: 569 cases (2002). JAVMA 225, 1084–1089.

Shaman, J., Day, J.F., Stieglitz, M., 2005. Drought-induced amplification and epidemic transmission of West Nile virus in Southern Florida. J. Med. Entomol. 42, 134–141.

Thomas, D.M., Urena, B., 2001. A model describing the evolution of West Nile-like encephalitis in New York City. Math. Comp. Mod. 34, 771–781.

Trock, S.C., Meade, B.J., Glaser, A.L., Ostlund, E.N., Lanciotti, R.S., Kropp, B.C., Kulasekera, V., Kramer, L.D., Komar, N., 2001. West Nile virus outbreak among horses in New York state, 1999 and 2000. Emerg. Infect. Dis. 7, 745–747.

USCB, 2010a. U.S. Census Bureau, Population Devision: Annual Estimates of the Resident Population for Counties of Minnesota. Available at: http://www.census.gov/popest/counties/CO-EST2009-01.html.

USCB, 2010b. U.S. Census Bureau: State & County Quick Facts. Available at: http://quickfacts.census.gov.

USDA, 2010. U.S. Department of Agriculture: National Agriculture Statistics Service, Census Quick Stats. Available at: http://quickstats.nass.usda.gov/.

USGS, 2010. U.S. Geological Survey: West Nile Virus Disease Maps. Available at: http://diseasemaps.usgs.gov/wnv_us_human.html.

Volz, E.M., Pond, S.L.K., Ward, M.J., Brown, A.J.L., Frost, S.D.W., 2009. Phylodynamics of infectious disease epidemics. Genetics 183, 1421–1430.

Ward, M.R., Stallknecht, D.E., Willis, J., Conroy, M.J., Davidson, W.R., 2006. Wild bird mortality and West Nile virus surveillance: biases associated with detection, reporting, and carcass persistence. J. Wildlife Dis. 42, 92–106.

Watson, J.T., Pertel, P.E., Jones, R.C., Siston, A.M., Paul, W.S., Austin, C.C., Gerber, S.I., 2004. Clinical characteristics and functional outcomes of West Nile fever. Ann. Intern. Med. 141, 360–365.

Weissenböck, H., Kolodziejek, J., Url, A., Lussy, H., Rebel-Bauder, B., Nowotny, N., 2002. Emergence of Usutu virus, an African mosquito-borne flavivirus of the Japanese encephalitis virus group, central Europe. Emerg. Infect. Dis. 8, 652–656.

Wonham, M.J., de Camino-Beck, T., Lewis, M.A., 2004. An epidemiological model for West Nile virus: invasion analysis and control applications. Proc. R. Soc. Lond. B 271, 501–507.

Wonham, M.J., Lewis, M.A., Renclawowicz, J., van den Driessche, P., 2006. Transmission assumptions generate conflicting predictions in host-vector disease models: a case study in West Nile virus. Ecol. Lett. 9, 706–725.

Yaremych, S.A., Warner, R.E., Mankin, P.C., Brawn, J.D., Raim, A., Novak, R., 2004. West Nile virus and high death rate in American crows. Emerg. Infect. Dis. 4, 709–711.